Modest diatom responses to regional warming on the southeast Tibetan Plateau during the last two centuries

Juliane Wischnewski[1,2*], Anson W. Mackay[3], Peter G. Appleby[4], Steffen Mischke[2], Ulrike Herzschuh[1,2]

[1] *Alfred Wegener Institute for Polar and Marine Research, Telegrafenberg A 43, 14473 Potsdam, Germany*

[2] *Institute of Earth and Environmental Sciences, University of Potsdam, Karl-Liebknecht-Str. 24, 14476 Potsdam-Golm, Germany*

[3] *Environmental Change Research Centre, Department of Geography, University College London, Pearson Building, Gower Street, London, WC1E 6BT, U.K.*

[4] *Department of Mathematical Sciences, University of Liverpool, Liverpool L69 3BX, UK*

[*] *Author for correspondence (Juliane.Wischnewski@awi.de)*

Key words: Diatoms, Tibetan Plateau, Mountain lake, Climate change, Lake sediments, Palaeolimnology

Abstract

A general mean annual temperature increase accompanied with substantial glacial retreat has been noted on the Tibetan Plateau during the last two centuries but most significantly since the mid 1950s. These climate trends are particularly apparent on the southeastern Tibetan Plateau. However, the Tibetan Plateau (due to its heterogeneous mountain landscape) has very complex and spatially differing temperature and precipitations patterns. As a result, a dense network of palaeolimnological investigations is necessary to decipher these climatic patterns and to understand ecological responses to recent environmental change. Here we present palaeolimnological results from a $^{210}Pb/^{137}Cs$ dated sediment core from a remote high mountain lake (LC6 Lake, working name) on the southeastern Tibetan Plateau spanning approximately the last 200 years. Sediment profiles of diatoms, organic parameters (TOC, C:N) and grain size were investigated. The ^{210}Pb record suggests a period of rapid sedimentation, which might be linked to major tectonic events in the region ca. 1950. Furthermore, unusually high ^{210}Pb supply rates over the last 50 years suggest that the lake has possibly been subjected to increasing precipitation rates, sediment focussing and/or increased spring thaw. The majority of diatom taxa encountered in the core are typical of slightly acidic to circumneutral, oligotrophic, electrolyte-poor lakes. Diatom species assemblages were rich, and dominated by *Cyclotella* sp, *Achnanthes* sp., *Aulacoseira* sp. and Fragilarioid taxa. Diatom compositional change was minimal over the 200-year period (DCCA = 0.85 SD, p = 0.59); only a slightly more diverse but unstable diatom assemblage was recorded during the past 50 years. The results indicate that large-scale environmental changes recorded in the 20th century (i.e. increased precipitation and temperatures) are likely

having an affect on the LC6 Lake, but so far these impacts are more apparent on the lake geochemistry than on the diatom flora. Local and/or regional peculiarities, such as increasing precipitation and cloud cover, or localized climatic phenomena such as negative climate feedbacks, may have off-set the effects of increasing mean surface temperatures.

Introduction

The Tibetan Plateau region is generally considered to be highly sensitive to climate change associated with global warming. The majority of meteorological stations across the Tibetan Plateau indicate a recent significant rise in both mean annual and mean winter surface temperatures (Liu and Chen 2000), resulting in permafrost degradation (Wu and Zhang 2008), and the acceleration of melting glaciers (Su and Shi 2002). However, the Tibetan Plateau is known for its highly complex temperature and moisture patterns in relation to its heterogeneous mountain landscape (An et al. 2000; Niu et al. 2004; You et al. 2010). In the densely populated monsoon region of south Asia, understanding temperature and moisture patterns in the past is crucial to help better estimate impacts of future climate variability. Several palaeoclimate studies have therefore been undertaken across the Tibetan Plateau, focussing on the Holocene time period (Herzschuh et al. 2009; Kramer et al. 2010). However, few studies have investigated environmental changes on the Tibetan Plateau during the last two centuries – a time period also strongly affected by increasing urbanisation and agricultural activity.

Ice core records from all regions of the Tibetan Plateau (Dasuopu, East Rongbuk, Puruogangri, Guliya, and Dunde ice core) point to a general warming trend over the past 200 years (Thompson et al. 1989; Thompson et al. 2000; Thompson et al. 2006; Yang et al. 2006; Hou et al. 2007). However, focussing on individual regions of the plateau, differences in temperature and precipitation trends become apparent. On the southeastern Tibetan Plateau (i.e. provinces of western Sinchuan, northwestern Yunnan and the easternmost part of the Tibet autonomous region), where conditions are semi-humid, a few tree ring studies exist, providing partly contradictory

information on climate trends of the recent past for this region (Bräuning and Mantwill 2004; Liang et al. 2009, Fan et al. 2010). Bräuning and Mantwill (2004) reconstructed a general increase in Indian summer monsoon activity after 1980 A.D. in their study area, although regional differences were noted in terms of temperature trends. For example, some growth regions on the southeastern Tibetan Plateau were indicative of warmer temperatures whereas other growth regions suggested cooler temperatures from 1970-1990 A.D.. Liang et al. (2009) found that the last decade (1996 – 2006) represents the warmest period since 1765 A.D., indicated by their tree ring width chronologies. In arid southern Tibet, ostracode and isotope studies suggest that a dry and cold climate prevailed between ca. 1600 – 1800 A.D.. After ca. 1800 A.D. the climate became more variable. Lake levels rose until ca. 1920 A.D., declined thereafter, and rose again from ca. 1970 A.D. until present (Wrozyna et al. 2010). In contrast, on the northwestern Tibetan Plateau, relatively dry conditions prevailed between ca. 1700 – 1900 A.D., followed by a wet phase from ca. 1900 – 1960 A.D., and a return to dryer conditions since 1960 A.D. (Henderson et al. 2003). Lami et al. (2010) analysed the geochemistry and algal pigments of different lakes across the Tibetan Plateau to assess the variability of trophic conditions over the last ca. 100 years. They found that six out of eight lakes show a marked increase in lake productivity within the last 100 years, which they attribute to climatic warming and land-use changes. In summary, information on relations between climate patters during the last two centuries and aquatic ecosystem responses is sparse and partly variable for the Tibetan Plateau.

Diatoms have shown to be useful indirect indicators for past environmental conditions by responding to limnological (biotic and abiotic) changes triggered by a changing climate (Douglas and Smol 2001; Lotter et al. 2001). Numerous diatom-

based palaeolimnological studies, with a focus on the last 100 – 200 years, have shown that alpine and arctic lakes are highly sensitive to changes in air temperature and precipitation. These studies are increasingly used to detect recent environmental change often associated with global warming (Lotter et al. 2002; Sorvari et al. 2002; Jones and Birks 2004; Solovieva et al. 2005; Rühland et al. 2008).

Here we present results from a $^{210}Pb/^{137}Cs$ dated sediment core from a remote high mountain lake (LC6 Lake) on the southeastern Tibetan Plateau spanning the last ~ 200 years. Sediment profiles of diatoms, organic parameters (TOC, C:N) and grain size were investigated. The aim of the paper is to examine the diatom response over a period of environmental change associated with generally significant temperature and precipitation increases and glacial retreat. As such, the paper exhibits one of the very few diatom records in the region and provides insights into the complexity of environmental change on the Tibetan Plateau.

Study site

The mountain lake (not named, working name LC6 Lake) is located in the Nyaintêntanglha Mountain range, on the southeastern Tibetan Plateau (Fig. 1). This mountain range is part of a large granite batholith in the interior of the plateau (Liu et al. 2004). The region is affected by two major circulation systems. The mid-altitude westerly circulation brings limited moisture to the region from November to March, while the South Asian Monsoon circulation is responsible for the majority of precipitation from May to September. This interplay results in abundant rainfall and high temperatures in summer, which is in contrast to the prevailing cool and relatively dry winters. The LC6 Lake lies at 4230 m above sea level (a.s.l.). The closest weather

station is in Nyingchi at 3000 m a.s.l., 26 km to the south of the lake, which records mean T_{July} 15.6°C, mean T_{Jan} 0.2°C, and mean P_{ann} 657mm (85% of P_{ann} falling between May and September). Based on a lapse rate of - 0.5°C/100 m (Böhner 2006), we estimate mean $T_{July} \sim 9.6$°C and mean $T_{Jan} \sim -5.5$°C in the LC6 Lake region. Following calculations derived from Böhner (2006), annual precipitation is estimated to be about 1450 mm, and evaporation rates around 800 mm at the lake site. According to the mean monthly temperature profile and monthly satellite images from the Landsat archive (USGS earth explorer) we estimate an ice cover duration on the lake of ~ 4 months (December – March).

General information about the lake and its catchment are summarised in Table 1. The LC6 Lake has a small lake area of 0.6 km^2 and is mainly fed by runoff from surrounding moderately steep-sloping mountains which generally peak around 4700 m a.s.l. The lake has one outflow, which cascades into a lake on a lower level to the southwest. With a maximum depth of 23 m, an approximate ice cover duration of 4 months, and a summer surface water temperature of 10.3°C (measured on 21.08.2005) the lake is likely to mix at least once a year (spring/summer) after winter stratification. The vegetation in the catchment is characterised by dense *Rhododendron* shrubs and coniferous forests (*Picea likiangensis* var. *balfouriana* (Rehder & Wilson) Hillier, *Abies georgei* var. *smithii* ((Viguié & Gaussen) Cheng, Cheng & Fu), and patches of *Kobresia pygmaea* (Clarke) Clarke meadow. Lichens are also typical epiphytes on surrounding shrubs and trees. No signs of immediate, catchment-scale human impact was observed during fieldwork, suggesting that LC6 Lake is particularly suitable to highlight possible effects of climate change.

Materials and Methods

Field sampling, sediment dating, physical and chemical data

In summer 2005, a 45-cm sediment core was taken at the deepest part (23 m) of LC6 Lake using a Glew gravity corer. The core was sectioned on site at 0.5-cm intervals directly after coring. For dating, sediment subsamples were analysed for ^{210}Pb, ^{226}Ra, and ^{137}Cs by direct gamma assay in the Liverpool University Environmental Radioactivity Laboratory. Radiometric dates were calculated using both the constant rate of supply (CRS) and constant initial concentration (CIC) ^{210}Pb dating models (Appleby and Oldfield 1978). Discrepancies between the ^{210}Pb models were resolved using the methods described in Appleby (2001). The 1963 depth was determined from the ^{137}Cs stratigraphic record. Dates of points below the base of the unsupported ^{210}Pb record were estimated by extrapolation of the ^{210}Pb depth/age curve using a best estimate of the sedimentation rate for this part of the core.

Total carbon, total nitrogen and total organic carbon (TOC) content of 47 sediment subsamples, with a constant spacing of 0.5 cm, were measured with a vario EL III elemental analyser. TOC was used as a parameter for describing the abundance of organic matter in the sediments and C:N ratio was calculated to examine the relative importance of autochthonous and allochthonous sources of organic material within the sediment core. Grain size analysis was performed with a Beckmann Coulter LS 200 laser particle analyser on 47 organic and carbonate-free subsamples at 0.5-cm spacing. Grain size parameters (calculated according to Tucker (1988)) were analysed to gain information on the sediment source and possible support in

understanding the age depth model (using peaks in the sand fraction as an indication of a stronger or sudden in-wash from the catchment or lake basin).

Diatom analysis

Diatom sample preparation followed standard procedures using the water bath technique (Renberg 1990; Battarbee et al. 2001). Slides were mounted using the mounting medium Naphrax®. Diatom concentration was estimated using DVB microspheres (Battarbee and Kneen 1982). Between 400 and 500 diatom valves were counted at x 1000 magnification. Taxonomic identifications primarily followed Krammer and Lange-Bertalot (1986 -1991), Lange-Bertalot and Metzeltin (1996), Camburn and Charles (2000), and Zhu and Chen (2000). A full list of taxonomic names, corresponding authority and the synonyms of previously accepted names are provided as supplementary data (Table S1). In our stratigraphy we chose to merge *Aulacoseira distans* (Ehrenb.) Simonsen with its varieties *A. distans* var. *nivalis* (Smith) Haworth and *A. distans* var. *nivaloides* Camburn as they were difficult to distinguish even under high magnification and showed similar trends. Small benthic Fragilarioid taxa (*Fragilaria spinarum* L-B & Metzeltin, *Staurosira construens* var. *venter* (Grun.) Williams & Round, *Staurosira construens* var. *binodis* (Ehrenb.) Hamilton, *Staurosira pinnata* (Ehrenb.) Williams & Round, *Pseudostaurosira pseudoconstruens* (Marciniak) Williams & Round) were also amalgamated as they have similar ecological preferences (Lotter and Bigler 2000) and showed similar trends. Diatoms are expressed as percent relative abundance of the total number of valves counted in each sample.

Numerical methods

Diatom-based biostratigraphic zones were identified by cluster analysis using constrained incremental sum of squares (CONISS) and the Edwards and Cavalli-Sforza's chord distance as the dissimilarity coefficient. Multivariate ordination techniques were undertaken on diatom species that were present with an abundance of 1% or greater in at least one sample. The main gradients of floristic variation in the diatom data were initially assessed using detrended correspondence analysis (DCA). As the gradient length of the first axis was only 1.08 standard deviation (SD) units, the linear ordination model of principal components analysis (PCA) was chosen for subsequent analysis (Lepš and Šmilauer 2003). PCA was preformed on a correlation matrix; species were centered and square-root transformed to stabilise their variance. Samples from the slump deposit between 27 cm - 8 cm core depth (see chronology results) are available as supplementary data only. Detrended canonical correspondence analysis (DCCA) was used to estimate the overall species turnover measured in SD units, which provides an estimate of compositional change along an environmental or temporal gradient (ter Braak and Verdonschot 1995). To estimate the amount of compositional change in our record in the last ~200 years, ^{210}Pb derived samples ages were used as the only constraining variable in DCCA. The decision whether the compositional turnover in our record is ecologically significant is based on the same protocols used by Smol et al. (2005). They used identical protocols to compare beta-diversity (compositional species turnover) in their Arctic sites to the beta-diversity in a set of reference sites (records from non-arctic, relatively unimpacted lakes) and established that changes greater than 1 SD unit were deemed ecologically substantial. In DCCA, species data were square-root transformed, no rare

species down-weighting was applied, and non-linear rescaling and detrending by segments was used. All ordinations were preformed using the program CANOCO 4.5 for Windows (ter Braak and Šmilauer 2002).

Diatom diversity was calculated for each sample using the Hill N_2 statistic (or inverse Simpson index), which is an estimate of the effective number of taxa in each sample. Species richness was estimated using rarefaction analysis, a method to standardise and compare species richness from samples of different size (Heck et al. 1975). However, changes in diatom diversity and species richness have to be viewed with caution, as variations in sedimentation rates and sediment compaction towards the base of the core, may falsify their interpretation (Smol 1981). Calculations for diatom diversity and species richness were carried out in R (R Development Core Team 2008) using the vegan package (Oksanen et al. 2008).

Results

Dating

For detailed illustration of the fallout radionuclides see Fig. 2. The results of the radiometric dating are summarised in Fig. 3a. The ^{210}Pb record is rather unusual in that although high concentrations in the near surface layers suggest an intrinsically low sedimentation rate, total ^{210}Pb activity exceeds that of the supporting ^{226}Ra down to a depth of 38 cm. Three distinct zones can be identified. Unsupported concentrations decline steeply with depth in the top 10 cm, reaching very low levels between 11.4-14.4 cm. Below this there is a zone of higher and relatively uniform concentrations, extending down to a depth of 30 cm. Below 30 cm unsupported concentrations decline at a rate comparable to that in the upper section of the core, falling below the limit of detection at around 38 cm (Fig. 2a, 2b). In contrast, the ^{137}Cs record is very conventional (Fig. 2c). Concentrations of this artificial radionuclide have a well defined peak in the 6.0-6.6-cm section that almost certainly records the 1963 fallout maximum from the atmospheric testing of nuclear weapons. Raw ^{210}Pb dates calculated using the CRS dating model alone suggest that the very low ^{210}Pb concentrations between 11.4-14.4 cm record an episode of extremely rapid sedimentation (Fig. 3a). There was however a significant discrepancy between the ^{210}Pb dates and the very well defined 1963 ^{137}Cs date, most probably due to the deposition of substantial amounts of additional ^{210}Pb during the course of this extreme event, possibly triggered by a landslide or within-lake sediment slump. Revised CRS model calculations for the upper part of the core using the ^{137}Cs date as a reference point (Appleby 2001) suggest that this event occurred in the late 1940s or early 1950s

and that since then sedimentation rates have been relatively uniform with a mean value of 0.15 cm y^{-1}. Even though rapid accumulation was most intense in those sediments between 11.4-14.4 cm, ^{210}Pb calculations suggest that the entire section of the core between 8 and 27 cm was deposited during the course of this event. Given this evidence, we have chosen to treat samples from the core section between 8-27 cm depth passively in subsequent statistical analyses. Calculations using the CIC model (Fig. 3a) indicate that sedimentation rates in the ^{210}Pb zone below 30 cm were similar to those in the post-1950 sediments, and hence that apart from the above episode, dry mass sedimentation rates (g cm^{-2} y^{-1}) at the core site have been relatively uniform during much of the past 100 years.

Based on these results, dates were extrapolated back to ca. 1800 A.D. Because of sediment compaction, the volumetric sedimentation rate (cm y^{-1}) during the earlier period used in these calculations (0.11 cm y^{-1}) was however a little lower than for the more recent sediments.

Grain size, TOC, and C:N ratio

The grain size distribution is relatively uniform throughout the core with silt being the dominating grain size fraction (65-83%) and the sand and clay fraction both contributing with ~11%. However, there are two distinct peaks in the sand fraction, accompanied by decreasing clay and silt values, at 28-23 cm and 9-8 cm core depth with the sand fraction rising to 26% and 23%, respectively (Fig. 3b). The TOC content separates the core into three sections (Fig. 3c). The bottom section of the core (45-29 cm) is marked by TOC values between 3.6 - 4.6 weight %, the middle section (29-8 cm) with lowest TOC values between 2.7 - 3.5 weight %, and the top section (8-

0 cm) has highest values ranging between 4.1 - 5.1 weight %. The C:N ratio (Meyers and Lallier-Vergès 1999) was calculated with the weight % of TOC and total N and shows relative constant values around 10 from 45-6 cm (until 1963) of the core. Thereafter, the C:N ratio declines steadily to ~ 8.5 at the top of the core (Fig. 3c).

Fossil diatom assemblage and numerical analysis

In the sediment core, a total of 158 species from 39 genera were identified (see Table S1 for full species list). The majority of taxa found in the core are typical of slightly acidic to circumneutral, oligotrophic, electrolyte-poor lakes and many are cosmopolitan species that are commonly found in freshwaters of nordic and alpine regions (Lotter and Bigler 2000; Sorvari et al. 2002; Rühland and Smol 2005). The most common taxa are monoraphid taxa (*Achnanthidium*, *Achnanthes* and *Psammothidium)*, *Cyclotella* and Fragilarioid taxa contributing to the diatom assemblage with up to 40%, 35% and 20% relative abundance, respectively. The most common species is the planktonic diatom *Cyclotella ocellata* (up to 35%). Changes in the relative abundances of all species throughout the core are minor. A subtle but consistent decline of *Cyclotella ocellata* (5-10%) is shown, accompanied by small increases in *Achnanthidium minutissimum* (Kutz.) Czarnecki,, tychoplanktonic *Aulacoseira lirata* var. *lirata* (Ehrenb.) Ross and benthic *Fragilaria capucina* Desmazières and *Cymbella* sp. This trend in diatom compositional changes is related to equally subtle changes in diatom diversity (N2), which is highest in recent decades. These minor changes are mainly driven by a modest increase in *Aulacoseira* taxa concurrent with an equally modest decrease in *Cyclotella ocellata*. DCCA revealed a compositional change of 0.85 SD (p= 0.59). The cluster analysis CONISS calculated a

total sum of squares of 1.8 and therefore no distinct first-order diatom biostratigraphic zones. The total diatom concentration in the pre- and post-slump deposit phase appears relatively stable with around 100 000 valves/g dry sediment. However, diatoms are more concentrated during the slump deposit with 250 000-550 000 valves/g dry sediment. Although minor, the diatom changes were most apparent before the 1880s and then again post 1960s. These subtle trends are summarised by PCA sample scores, which indicate that the unstable diatom assemblage after the 1960s is linked to monoraphid and *Aulacoseira* species (Fig. 5). PCA ordination results show that the main gradient is along the first component, accounting for 24% of the variation in the diatom data set and dividing the data set in taxa stronger associated with the phase of the sediment slump from taxa occurring in the post-slump phase. The second axis accounts for 10% of the variance in the data set and represents the gradient between taxa pre- and post- 1950 AD. The most common diatoms and diatom functional groups are plotted stratigraphically and are compared to summaries of diatom compositional changes (PCA1 and PCA 2 samples scores), species turnover (DCCA 1), species diversity, and relative changes of planktonic, tychoplanktonic and benthic components (Fig. 4).

Discussion

Radiometric evidence for irregular sedimentation events and increasing sedimentation during recent decades

Low ^{210}Pb concentrations between 8 – 27 cm, the down-core TOC content, and grain size distribution suggest that this core section was most likely accumulated during the course of one single rapid event, possibly a landslide or, more likely, a within-lake sediment slump. The increase diatom concentration during that period suggests that a large component of the sediment slump comes from diatom-rich sediments from the slopes surrounding the core site. The relative small decline in TOC and small peak in the sand fraction further suggest that the sediment input is not solely from clastic rich sediments. The age model suggests that this event happened between the late 1940s and early 1950s. This interpretation correlates very well with the timing of the Assam-Tibet earthquake that was recorded in August 1950, in North India, just ~ 280 km southeast to the site. Strasbourg calculated a magnitude of 8.6 on the Richter scale and classified the quake as one of the most important since the introduction of seismological observing stations. Ground motion could be felt from Lhasa to Calcutta (USGS earthquakes). Additionally, diatom samples from the 8-27-cm section plot within the same cluster in the PCA (Fig. 5), suggesting that species composition in this core section is very similar.

Even during the periods of uniform sedimentation, supply rates of ^{210}Pb are unusually high. The mean value (calculated from the post-1963 ^{210}Pb inventory) is well in excess of the values obtained from other Tibetan lakes, and substantially higher than the atmospheric flux. Two possible reasons for this are that the core is

from a site in the lake subject to intense sediment focusing, or that substantial quantities of ^{210}Pb deposited in the catchment are transported into the lake during spring thaw. This is partially supported by instrumental climate data from the region, which indicate increasing precipitation rates and rising winter and spring temperatures over the last ~50 years (Lui and Chen 2000, You et al. 2007), possibly leading to higher input rates of ^{210}Pb.

Diatom response to recent environmental changes on the southeast Tibetan Plateau

The minimal diatom compositional changes over the 200-year period (<1SD) is according to established standards from Smol et al. (2005) ecologically insignificant. Similar low SD values were calculated for diatom records from northern Quebec, where diatom compositional change in agreement with instrumental data suggest no significant warming over the past 150 years (Smol et al. 2005).

Many studies on lakes in Arctic (Sorvari et al 2002; Rühland et al. 2003; Jones and Birks 2004; Smol et al. 2005; Solovieva et al. 2005; Holmgren et al. 2010) and alpine (Lotter and Bigler 2000; Koinig et al. 2002; Lotter et al. 2002) environments, however, have detected a significant shift from benthic to planktonic dominated assemblages around 1850 A.D., as a result of longer ice-free periods linked to global warming after the end of the Little Ice Age. In these studies, earlier ice break up, triggered by rising mean winter and spring temperatures, would lead to a longer growing season and changes in the light and mixing regime and increased nutrient cycling that in turn would enhance especially planktonic growth. Hence, recent warming trends detected in temperate regions of the Northern Hemisphere and were accompanied by a significant shift from benthic (e.g. small Fragilarioid species as

well as heavily silicified *Aulacoseira* taxa) to planktonic (e.g. small *Cyclotella* species) taxa (Rühland et al. 2008).

Similar to many Arctic and alpine regions of the world, an overall increase in temperature has been recorded on the Tibetan Plateau after the end of the Little Ice Age and post 1960 (Thompson et al. 2000; Hou et al. 2007). Continuous meteorological data for the Tibetan Plateau is available from the mid-1950s to the present and indicate an increase in mean winter temperatures of 0.16°C/decade between 1955 and 1996 (Liu and Chen 2000). You et al. (2007) analysed meteorological temperature and precipitation data from 10 stations in the Yarlung Zangbo River Basin and found similar climatic trends to our study area, indicating increasing mean winter and autumn temperatures of 0.37°C and 0.35°C/decade, respectively since 1961. Furthermore, You et al. (2007) identified a decreasing precipitation trend from the 1960s to the 1980s but a rising precipitation trend since the 1980s, which is most obvious in the autumn and spring season. According to their findings, Chen and Lui (2000) and You et al. (2007) suggest that particularly the southeastern Tibetan Plateau is most sensitive to global warming.

It is evident that the Tibetan Plateau is experiencing substantial warming over the recent past. With rising temperatures we would expect a shortening in the ice cover length. However, the shift to warmer and moister conditions is not manifested in our diatom record from LC6 Lake. Species compositional changes are very subtle and a clear shift from benthic to planktonic taxa was not be observed. In contrast, we found a directional decline (5-10%) in planktonic taxa, mainly *Cyclotella ocellata*, throughout the core, while benthic taxa show a small increase. PCA sample scores from the base of the core to approx. 1870 A.D. summarise changes in the diatom assemblage and may indicate post-Little Ice Age warming.. However, all of these

changes are likely ecologically insignificant. More apparent is the increase in the relative abundance of tychoplanktonic taxa (*Aulacoseira distans* and varieties, *Aulacoseira lirata var. lirata),* small Fragilarioid taxa and *A. minutissimum* since the mid- 1950s, which is coherent with a minor increase in species richness and N2 diversity. TOC shows a modest increase whilst the C:N ratio declines moderately. Higher TOC in recent decades points to an overall increase in lake productivity, while C:N indicates an increased importance of algal productivity in the lake. Lami et al. (2010), found decreasing C:N ratios across Tibetan lakes over the last decades, which they link to climate warming and recent anthropogenic land-use changes. As no immediate, catchment-scale human impact is noticeable at our site, higher nutrient availability probably arises from changes in nutrient cycling linked to changes in the ice cover length (Douglas and Smol 2001) or increased meltwalter input from upstream glaciers. The presence of tychoplanktonic taxa at LC6 Lake and the growing importance of Fragilarioid taxa, which are known to be *r*-strategists and therefore better adapted to rapid changing environments (Lotter and Bigler 2000) is indicative of higher ecosystem variability. Higher ecosystem variability during this time was also recorded in other palaeo-climate records across the Tibetan Plateau (Yang et al. 2004; Lami et al. 2010; Wrozyna et al. 2010). Major changes in the diatom concentration occur only in the sediment slump deposit and probably represent an artefact due to the change in the sedimentation rate. Variability in the diatom concentration throughout the rest of the record was tested insignificant. Overall, the stability of the LC6 diatom assemblages throughout the core is indicative of very little change within the lake over the past ca. 200 years and it seems prudent to further examine possible reasons for the apparent insensitivity of the diatom assemblage towards environmental changes on the southeastern Tibetan Plateau.

Possible reasons for a modest diatom response to recent environmental change

You et al. (2010) argue that increasing temperatures are not necessarily correlated with elevation. In contrast to earlier studies (Lui and Chen 2000), they argue that the significant temperature increases that are recorded from climate stations at 2500- 3000 m a.s.l., are not as pronounced at climate stations at higher altitudes. According to Pepin and Lundquist (2008), the highest temperature changes appear at the 0°C isotherm where melting of snow and ice influences the surface albedo and consequently enhances further warming (cryosphere feedback). Nyingchi (3000 m a.s.l., mean T_{Jan} 0.2°C), the closest climate station to LC6 Lake (see Fig. 1), indicates a significant increase (approx. 1°C) in mean and minimum temperatures in all seasons since the 1960s (Liang et al. 2009). According to Pepin and Lundquist (2008) and You et al. (2010), the temperature trend magnitude at our site (4132 m a.s.l., mean $T_{Jan} \sim$ -5.5°C) could have been smaller or less significant than in Nyingchi (3000 m a.s.l.) due to reduced cryospheric feedback recorded at higher altitudes, possible explaining the lack for significant changes in the diatom record.

Furthermore, You et al. (2010) show that regions on the Tibetan Plateau with a low-growing vegetation type have larger temperature trend magnitudes than regions with denser vegetation. This may seem counter-intuitive, but on the Tibetan Plateau, areas with dense vegetation in combination with increasing precipitation may result in increased cloud cover and decreasing sunshine that may act to buffer the full effect of increasing temperatures. The very dense coniferous forests intermixed with *Rhododendron* in the catchment of LC6 could have acted as a temperature buffer. Dense epiphytic growth from lichens and mosses in these forests also indicate

permanent high moisture and cloud cover in the valley of LC6 Lake. Increasing precipitation, cloud cover and decreasing sunshine duration is also confirmed by instrumental data (Niu et al. 2004). Increasing precipitation rates and increased cloud cover might have antagonized increasing temperature and associated increasing evaporation trends in the area. This could explain the minimal changes observed in our diatom assemblages and likely the aquatic habitat (mixing, stratification, lake water depth). Increasing winter and spring precipitation rates, likely linked to the intensification of the westerlies over the southern slope of the Tibetan Plateau (Zhang et al. 2004), can further lengthen the ice cover duration and therefore counteract the tendency towards earlier ice melting as would be expected with increasing air temperatures (Lotter at el. 2002).

Another possibility for the limited diatom response is that the LC6 Lake possibly does not stratify (in summer), often a key factor in driving recent diatom changes reported around the globe (Sorvari et al. 2002; Rühland et al. 2008). Wind stress or smaller differences between summer and winter water temperature, in combination with increased precipitation and cloud cover could maintain a well-mixed water column, thus preventing major changes in habitat conditions and in diatom composition despite recent warming trends. Furthermore, one could argue that warming in one region may have negative feedbacks in other regions such as in the down-slope areas of glacier-covered and climate-sensitive mountain regions. Rühland et al. (2006) suggested that substantial increases in temperature in the Himalayas did not lead to the expected drying of the investigated peatland, but to a significant increase of moisture and maintenance of cooler conditions, triggered by the increased runoff of melting glaciers from the upstream regions. Su and Shi (2002) have recorded substantial glacial retreat on the southeastern Tibetan Plateau, especially in

the mountain range studied here. Increased melting and mountain runoff from peaks upstream of LC6 Lake may have provided a constant supply of cold glacial melt waters to our study site, off-setting the effects of warming lake surface water temperatures at LC6 Lake and preventing or weakening the potential for thermal stratification. Unusually high supply rates of ^{210}Pb support this hypothesis, indicating that substantial quantities of ^{210}Pb deposited in the catchment are transported into the lake during spring thaw.

To rule out the effect of a local climatic phenomenon that may have had an influence on the stability of the diatom composition, further palaeoecological investigations on the southeastern Plateau are necessary. Our results highlight the spatial complexity of climate change on the Tibetan Plateau, and indicate the need for widespread regional coverage of palaeo-ecological data in order to better understand the regional dynamics of future global change.

Acknowledgements

We would like to thank Chengjun Zhang (Lanzhou University) for his help during fieldwork; Vivienne Jones and Carl Sayer for helpful advice with diatom identification; and Ute Bastian for her support in the sediment lab. Comments and advice from Kathleen Rühland and one anonymous reviewer are greatly appreciated. This research was funded by a scholarship to J.W. as part of the German Research Council (DFG, Deutsche Forschungsgemeinschaft) graduate school GRK1364.

References

An Z, Porter S, Kutzbach J, Xihao W, Suming W, Xiaodong L, Xiaoqiang L, Weijian Z (2000) Asynchronous Holocene optimum of the East Asian monsoon. Quat Sci Rev 19: 743-762.

Appleby PG (2001) Chronostratigraphic techniques in recent sediments. In: Last WM, Smol JP (Eds.) Tracking Environmental Change Using Lake Sediments Volume 1: Basin Analysis, Coring, and Chronological Techniques. Kluwer Academic Publishers, Dordrecht.

Appleby PG, Oldfield F (1978) The calculation of 210Pb dates assuming a constant rate of supply of unsupported 210Pb to the sediment. Catena, 5:1-8.

Battarbee RW, Jones VJ, Flower RJ, Cameron NG, Bennion H, Carvalho L, Juggins S (2001) Diatom analysis. In: Last WM, Smol JP (eds) Tracking Environmental Change Using Lake Sediments, Vol. 3: Terrestrial, Algal and Silicieous Indicators. Kluwer Academic Publishers, Dordrecht.

Battarbee RW, Kneen MJ (1982) The use of electronically counted microspheres in absolute diatom analysis. Limnol Oceanogr: 184-188.

Böhner J (2006) General climatic controls and topoclimatic variations in Central and High Asia. Boreas 35: 279-295.

Bräuning A, Mantwill B (2004) Summer temperature and summer monsoon history on the Tibetan plateau during the last 400 years recorded by tree rings. Geophys Res Lett 31: L24205.

Camburn KE, Charles DF (2002) Diatoms of Low-Alkalinity Lakes in the Northeastern United States. The Academy of natural Sciences, Philadelphia.

Douglas MSV, Smol JP (2001) Freshwater diatoms as indicators of environmental changes in the High Arctic. In: Stoermer EF, Smol JP (eds) The Diatoms: Application for the Environmental and Earth Sciences. Cambridge University Press, Cambridge, pp 227-244.

Fan Z.-X., Bräuning A., Tian Q.-H., Yang B. and Cao K.-F. (2010) Tree ring recorded May–August temperature variations since A.D. 1585 in the Gaoligong Mountains, southeastern Tibetan Plateau. Palaeogeogr, Palaeocl, Palaeoecol 296: 94-102.

Heck KL, van Belle G, Simberloff D (1975) Explicit calculation of the rarefaction diversity measurement and the determination of sufficient sample size. Ecology 56: 1459–1461.

Henderson A, Holmes J, Zhang J, Leng M, Carvalho L (2003) A carbon-and oxygen-isotope record of recent environmental change from Qinghai Lake, NE Tibetan Plateau. Chin Sci Bull 48: 1463-1468.

Herzschuh U, Kramer A, Mischke S, Zhang C (2009) Quantitative climate and vegetation trends since the late glacial on the northeastern Tibetan Plateau deduced from Koucha Lake pollen spectra. Quat Res 71: 162-171.

Holmgren SU, Bigler C, Ingólfsson Ó,Wolfe AP (2010) The Holocene–Anthropocene transition in lakes of western Spitsbergen, Svalbard (Norwegian High Arctic): climate change and nitrogen deposition. J Paleolimnol 43: 393-412.

Hou S, Chappellaz J, Jouzel J, Chu P, Masson-Delmotte V, Qin D, Raynaud D, Mayewski P, Lipenkov V, Kang S (2007) Summer temperature trend over the past two millennia using air content in Himalayan ice. Climate Past 3: 89-95.

Jones V, Birks H (2004) Lake-sediment records of recent environmental change on Svalbard: results of diatom analysis. J Paleolimnol 31: 445-466.

Koinig K, Kamenik C, Schmidt R, Agustí-Panareda A, Appleby P, Lami A, Prazakova M, Rose N, Schnell Ø, Tessadri R (2002) Environmental changes in an alpine lake (Gossenköllesee, Austria) over the last two centuries–the influence of air temperature on biological parameters. J Paleolimnol 28: 147-160.

Kramer A, Herzschuh U, Mischke S, Zhang C (2010) Holocene treeline shifts and monsoon variability in the Hengduan Mountains (southeastern Tibetan Plateau), implications from palynological investigations. Palaeogeogr Palaeoclimatol Palaeoecol 286: 23-41.

Krammer K, Lange-Bertalot H (1986-1991) Bacillariophyceae, vol. 1-4. Gustav Fischer Verlag, Stuttgart.

Lami A, Turner S, Musazzi S, Gerli S, Guilizzoni P, Rose NL, Yang H, Wu G,Yang R (2010) Sedimentary evidence for recent increases in production in Tibetan plateau lakes. Hydrobiologia 648: 175-187.

Lange-Bertalot H, Metzeltin D (1996) Indicators of Oligotrophy. In: Lange-Bertalot H (Ed.) Iconographia Diatomologica: Annotated Diatom Micrographs, vol. 2. Koeltz Scientific Books, Königstein.

Lepš J, Šmilauer P (2003) Multivariate analysis of ecological data using CANOCO. Cambridge University Press, Cambridge.

Liang EY, Shao XM, Xu Y (2009) Tree-ring evidence of recent abnormal warming on the southeast Tibetan Plateau. Theor Appl Climatol 98: 9-18.

Liu X, Chen B (2000) Climatic warming in the Tibetan Plateau during recent decades. Int J Climatol 20: 1729-1742.

Liu Q, Wu Z, Hu D, Ye P, Jiang W, Wang Y,Zhang H (2004) SHRIMP U-Pb zircon dating on Nyainqentanglha granite in central Lhasa block. Chin Sci Bull 49: 76-82.

Lotter A, Bigler C (2000) Do diatoms in the Swiss Alps reflect the length of ice-cover? Aquat Sci 62: 125-141.

Lotter A, Pienitz R, Schmidt R (2001) Diatoms as indicators of environmental change near arctic and alpine treeline. In: Stoermer EF, Smol JP (eds) The Diatoms: Application for the Environmental and Earth Sciences. Cambridge University Press, Cambridge, pp 205-226.

Lotter A, Appleby P, Bindler R, Dearing J, Grytnes J, Hofmann W, Kamenik C, Lami A, Livingstone D, Ohlendorf C (2002) The sediment record of the past 200 years in a Swiss high-alpine lake: Hagelseewli (2339 m asl). J Paleolimnol 28: 111-127.

Meyers PA, Lallier-Vergès E (1999) Lacustrine sedimentary organic matter records of Late Quaternary paleoclimates. J Paleolimnol 21: 345-372.

Niu T, Chen L, Zhou Z (2004) The characteristics of climate change over the Tibetan Plateau in the last 40 years and the detection of climatic jumps. Adv Atmos Sci 21: 193-203.

Oksanen J, Kindt R, Legendre P, O'Hara B, Simpson GL, Solymos P, Stevens MHH, Wagner H (2008) Vegan: Community Ecology Package. R package version 1.15-1.

Pepin NC, Lundquist JD (2008) Temperature trends at high elevations: Patterns across the globe. Geophys. Res. Lett. 35: L14701.

R Development Core Team (2008) R: A language and environment for statistical computing. R Foundation for Statistical Computing, Vienna, Austria.

Renberg I (1990) A procedure for preparing large sets of diatom slides from sediment cores. J Paleolimnol 4: 87-90.

Rühland K., Priesnitz A. and Smol J.(2003) Paleolimnological evidence from diatoms for recent environmental changes in 50 lakes across Canadian Arctic treeline. Arct, Antarct, Alp Res 35: 110-123.

Rühland K, Smol J (2005) Diatom shifts as evidence for recent Subarctic warming in a remote tundra lake, NWT, Canada. Palaeogeogr Palaeocl Palaeoecol 226: 1-16.

Rühland K, Phadtare N, Pant R, Sangode S, Smol J (2006) Accelerated melting of Himalayan snow and ice triggers pronounced changes in a valley peatland from northern India. Geophys. Res. Lett. 33: L15709.

Rühland K, Paterson A, Smol J (2008) Hemispheric-scale patterns of climate-related shifts in planktonic diatoms from North American and European lakes. Glob Change Biol 14: 2740-2754.

Smol J. (1981) Problems associated with the use of `species diversity"in paleolimnological studies. Quat Res 15: 209-212.

Smol J, Wolfe A, Birks H, Douglas M, Jones V, Korhola A, Pienitz R, Ruhland K, Sorvari S, Antoniades D (2005) Climate-driven regime shifts in the biological communities of arctic lakes. P Natl Acad Sci 102: 4397-4402.

Solovieva N, Jones VJ, Nazarova L, Brooks SJ, Birks HJB, Grytnes JA, Appleby PG, Kauppila T, Kondratenok B, Renberg I (2005) Palaeolimnological evidence for recent climatic change in lakes from the northern Urals, arctic Russia. J Paleolimnol 33: 463-482.

Sorvari S, Korhola A, Thompson R (2002) Lake diatom response to recent Arctic warming in Finnish Lapland. Glob Change Biol 8: 171-181.

Su Z,Shi Y (2002) Response of monsoonal temperate glaciers to global warming since the Little Ice Age. Quatern Int 97-98: 123-131.

Ter Braak CJF, Šmilauer P (2002) CANOCO Reference Manual and CANODRAW for Windows User's Guide: Software for Canonical Community Ordination (Version 4.5). Microcomputer Power, New York.

Ter Braak CJF, Verdonschot PFM (1995) Canonical correspondence analysis and related multivariate methods in aquatic ecology. Aquat Sci 57: 255.

Thompson LG, Yao T, Davis ME, Mosley-Thompson E, Mashiotta TA, Lin PN, Mikhalenko VN, Zagorodnov VS (2006) Holocene climate variability archived in the Puruogangri ice cap on the central Tibetan Plateau. Ann Glaciol 43: 61-67.

Thompson L, Yao T, Mosley-Thompson E, Davis M, Henderson K,Lin P (2000) A high-resolution millennial record of the South Asian Monsoon from Himalayan ice cores. Science 289: 1916-1919.

Thompson LG, Mosley-Thompson E, Davis ME, Bolzan J, Dai J, Klein L, Yao T, Wu X, Xie Z, Gundestrup N (1989) Holocene-Late Pleistocene Climatic Ice Core Records from Qinghai-Tibetan Plateau. Science 246: 474.

Tucker ME (1988) Techniques in Sedimentology. Blackwell Scientific Publications.

USGS earthquakes. http://earthquake.usgs.gov/earthquakes/world/events/1950_08_15.php (last access: 16.02.2010)

USGS earth explorer. http://edcsns17.cr.usgs.gov/EarthExplorer/ (last access: 14.04.2010)

Wrozyna C, Frenzel P, Steeb P, Zhu L, Geldern Rv, Mackensen A, Schwalb A (2010) Stable isotope and ostracode species assemblage evidence for lake level changes of Nam Co, southern Tibet, during the past 600years. Quatern Int 212: 2-13.

Wu Q, Zhang T (2008) Recent permafrost warming on the Qinghai-Tibetan Plateau. J Geophys Res 113: D13108.

Yang X, Sumin W, Kamenik C, Schmidt R, Shen J, Liping Z, Shengfeng L (2004) Diatom assemblages and quantitative reconstruction for paleosalinity from a sediment core of Chencuo Lake, southern Tibet. Sci China Ser D 47: 522-528.

Yang M, Yao T, Wang H,Gou X (2006) Correlation between precipitation and temperature variations in the past 300years recorded in Guliya ice core, China. Annals of Glaciology 43: 137.

You Q, Kang S, Wu Y,Yan Y (2007) Climate change over the Yarlung Zangbo River Basin during 1961–2005. J Geogr Sci 17: 409-420.

You Q, Kang S, Pepin N, Flügel W-A, Yan Y, Behrawan H, Huang J (2010) Relationship between temperature trend magnitude, elevation and mean temperature in the Tibetan Plateau from homogenized surface stations and reanalysis data. Global Planet Change 71: 124-133.

Zhang Y, Li T,Wang B (2004) Decadal change of the spring snow depth over the Tibetan Plateau: The associated circulation and influence on the East Asian summer monsoon. J Climate 17: 2780-2793.

Zhu H, Chen J (2000) Bacillariophyta of the Xizang Plateau. Science Press, Beijing (in Chinese).

Zhu W, Chen L, Zhou Z (2001) Several characteristics of contemporary climate change in the Tibetan Plateau. Sci China Ser D 44: 410-420.

List of Tables

Table 1: Selected physical and chemical characteristics of LC6 Lake

LC6 Lake	
Latitude	29.82515
Longitude	94.45615
Elevation	4132m a.s.l.
Genesis	Glacial lake
Lake area	2000 x 300 m, ~ 0.6 km^2
Catchment area	~ 13.5 km^2
Max. water depth	23 m
Secchi depth	6.9 m
Conductivity	0.013 mS/cm
pH	7.0
Alkalinity	0.4 mmol/l
Inflow	Mountain runoff
Outflow	One cascading outlet into lake at lower level

Figure Captions

Fig. 1: a) Core position, outflow and catchment area (dashed line) of LC6 Lake, b) study site location; c) topography and location of LC6 Lake and other locations mentioned in the text. Figures adopted from Landsat and The Map Creation Tool. ATEQ (Assam-Tibet earthquake August 1950).

Fig. 2: Fallout radionuclides showing (a) total and supported ^{210}Pb, (b) unsupported ^{210}Pb, and (c) ^{137}Cs concentrations versus depth.

Fig 3a ,3b and 3c: Radiometric chronology showing the 1963 depth determined from the ^{137}Cs. The piecewise CRS model ^{210}Pb dates and sedimentation rates, and the CIC model ^{210}Pb dates calculated for those sections of the core above 7.5 cm and below 30 cm thought to represent periods of uniform accumulation (3a). Age chronology is compared with the grain size distribution (3b) and the TOC content and C:N ratio (3c).

Fig. 4: Diatom stratigraphy of the LC6 Lake. Selected taxa are shown in relative abundance and comparison with autecology, species richness, N2 diversity, ordination scores (PCA 1 and PCA 2, DCCA 1). Area between 8 and 28 cm refers to the slump deposit. Ages A.D. in italic font indicate extrapolated dates.

Fig. 5: Results of the Principle Component Analysis (PCA), showing diatom species with taxa >1% abundance. For species abbreviations see full species list in the supplementary data (Table S1). Solid black sample points were treated as passive samples as they form samples from the slump deposit. To ease visibility, species are

displayed as symbols only (but treated as vectors, as appropriate for linear methods). Dashed circles indicate the time periods pre-slump deposit, slump deposit and post-slump deposit.

Supplementary Data:

Table 1: Species list with authorities, Synonyms, and abbreviations. Asterisk indicates taxa with maximum relative abundance of <1%.

Figures

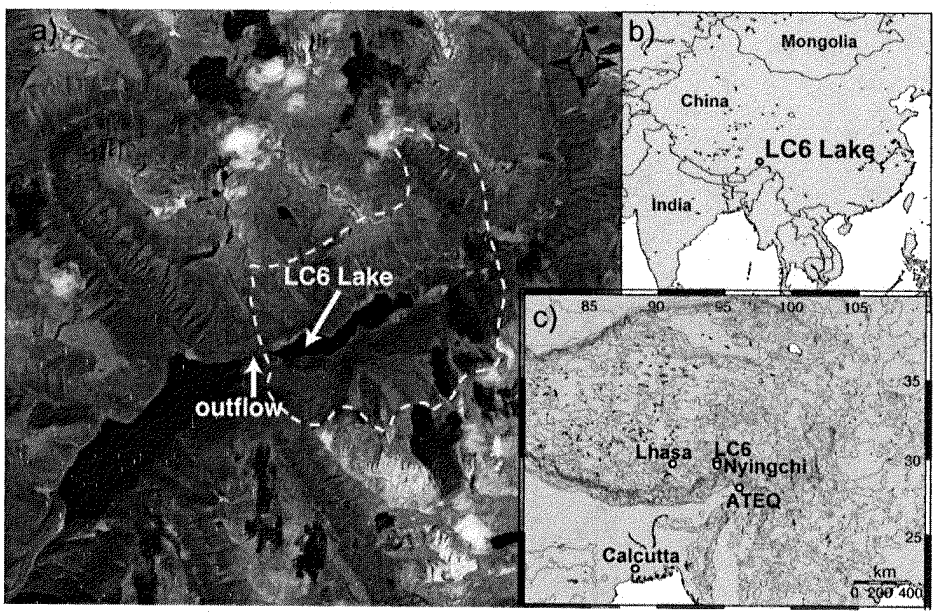

Figure 1

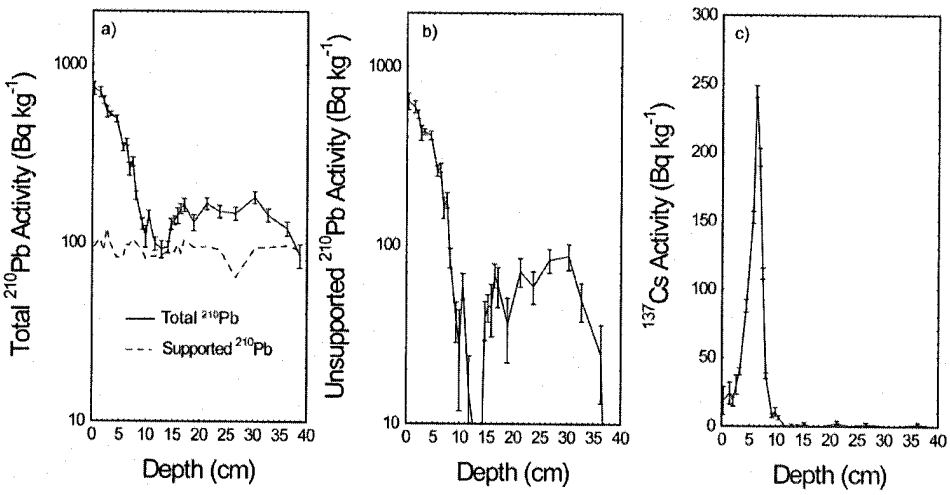

Figure 2

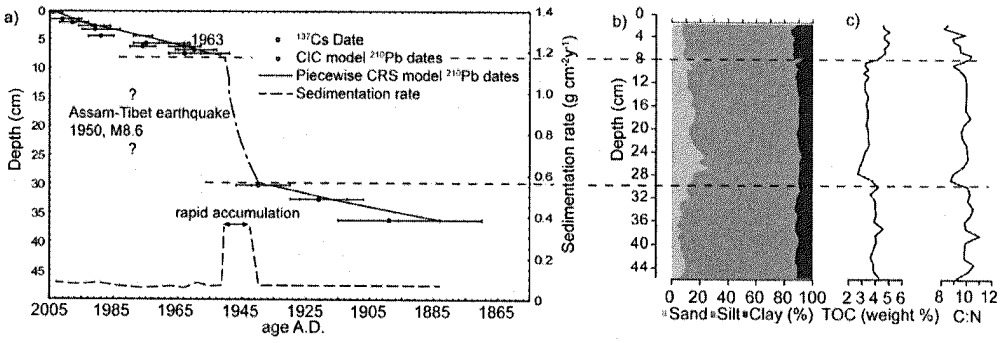
a)
b)
c)
1963
^{137}Cs Date
CIC model ^{210}Pb dates
Piecewise CRS model ^{210}Pb dates
Sedimentation rate
?
Assam-Tibet earthquake
1950, M8.6
?
rapid accumulation
Depth (cm)
Sedimentation rate (g cm^{-2}y^{-1})
age A.D.
2005 1985 1965 1945 1925 1905 1885 1865
Depth (cm)
0 20 40 60 80 100
Sand Silt Clay (%)
2 3 4 5 6
TOC (weight %)
8 10 12
C:N

Figure 3

783

784 Figure 4

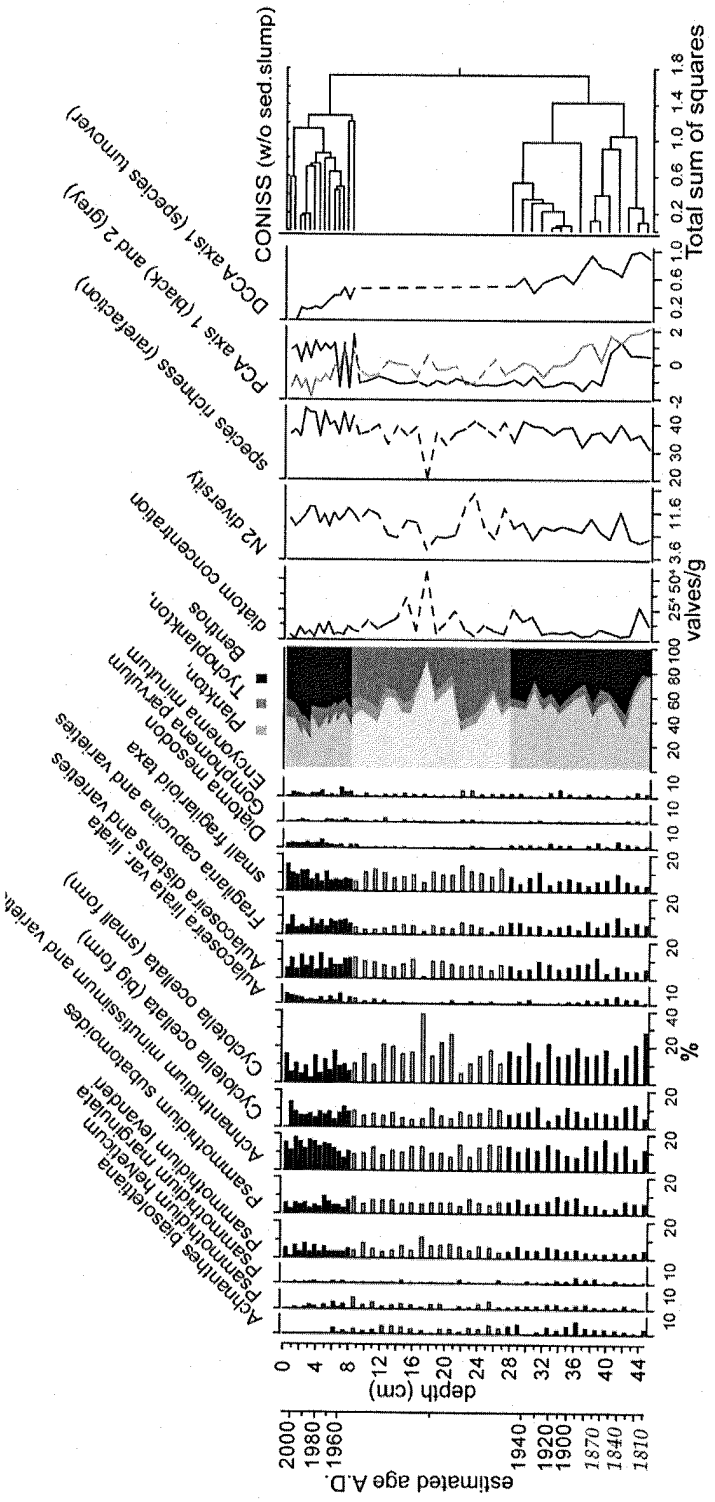

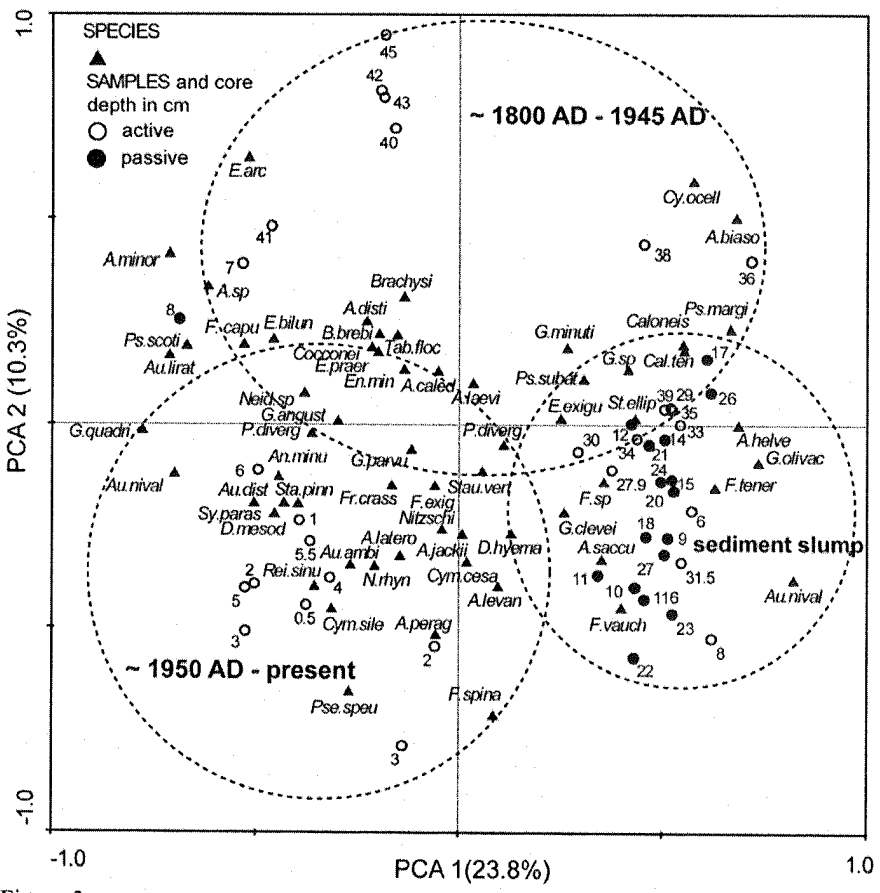
SPECIES
SAMPLES and core depth in cm
active
passive
~ 1800 AD - 1945 AD
~ 1950 AD - present
sediment slump
PCA 2 (10.3%)
PCA 1(23.8%)
1.0
-1.0
-1.0
1.0
E.arc
A.minor
A.sp
Brachysi
A.disti
F.capu
E.bilun
B.brebi
Tab.floc
Ps.scoti
Au.lirat
Cocconei
E.praer
En.min
A.calêd
Neidsp
G.angust
G.quadri
P.diverg
An.minu
G.parvu
Au.nival
Au.dist
Sta.pinn
Fr.crass
Stau.vert
F.exig
Sy.paras
D.mesod
Nitzschi
A.latero
Au.ambi
A.jackii
D.hyema
Rei.sinu
N.rhyn
Cym.cesa
A.levan
Cym.sile
A.perag
Pse.speu
F.spina
Cy.ocell
A.biaso
Ps.margi
Caloneis
G.minuti
G.sp
Cal.ten
Ps.subat
A.laevi
E.exigu
St.ellip
A.helve
G.olivac
F.tener
F.sp
G.clevei
A.saccu
Au.nival
F.vauch

Figure 5

789

Code	Species and Authority	Synonym	Abbreviaton in PCA
ACH0037B	**Achnanthes biasolettiana* Lange-Bertalot, 1989		A.biaso
ACH00XY1	*Achnanthes bremeyeri* Lange-Bertalot, 1989		A.breme
ACH00XY2	**Achnanthes caledonica* Lange-Bertalot & Moser, 1994		A.caled
ACH0023A	*Achnanthes conspicua* A. Mayer, 1919		A.consp
ACH0016C	*Achnanthes delicatula var.hauckiana* (Grun. in Cleve & Grun.) Lange-Bertalot & Ruppel, 1980		A.delic
ACH0039A	*Achnanthes didyma* Hust, 1933		A.didym
ACH0155A	**Achnanthes distincta* Messikommer, 1954		A.disti
ACH0163A	**Achnanthes helvetica* (Hustedt) Lange-Bertalot in LB & K, 1989		A.helve
ACH0134C	**Achnanthes helvetica var. minor* Flower & Jones, 1989		A.minor
ACH0170A	*Achnanthes joursacense* Herib., 1903		A.joura
ACH0149A	*Achnanthes kranzii* Lange-Bertalot & Krammer, 1989		A.kranz
ACH0017A	*Achnanthes kryophila* J.B. Petersen, 1924		A.kryo
ACH0083A	**Achnanthes laevis* Ostr., 1910		A.laevi
ACH0018A	**Achnanthes laterostrata* Hust., 1933		A.latero
ACH0044A	**Achnanthes levanderi* Hust., 1933		A.levan
ACH0013C	**Achnanthes minutissima var. jackii* (Rabenh.) Lange-Bertalot & Ruppel, 1980		A.jackii
ACH0098A	*Achnanthes montana* Krasske, 1929		A.monta
ACH0019A	*Achnanthes nodosa* A. Cleve-Euler, 1900		A.nodos
ACH0007A	*Achnanthes oestrupii* (A. Cleve-Euler) Hust, 1930		A.oestr
ACH0011A	**Achnanthes peragalli* Brun & Herib. in Herib., 1893		A.perag
ACH0182A	*Achnanthes rosenstockii* Lange-Bertalot, 1989		A.rosen
ACH0116A	*Achnanthes rossii* Hust, 1954		A.rossii
ACH0119A	**Achnanthes saccula* J.R. Carter in J.R. Carter & Watts, 1981		A.saccu
ACH9999A	**Achnanthes* species		A.sp
ACH0034A	*Achnanthes suchlandtii* Hust, 1933		A.suchl
ACH0161A	*Achnanthes ventralis* (Krasske) Lange-Bertalot, 1989		A.ventra
CAN0012A	*Achnanthidium minutissimum* (Kutz.) Czarnecki, 1994	*Achnanthes minutissima*	An.minu
AMP0010A	*Amphora fogediana* Krammer, 1985		Am.foge
AMP0013A	*Amphora inariensis* Krammer, 1985		Am.inari
AMP0011A	*Amphora libyca* Ehr., 1840		Am.liby
AMP0001A	*Amphora ovalis* (Kutz.) Kutz., 1844		Am.oval
AMP0012A	*Amphora pediculus* (Kützing) Grunow, in Schmid et al., 1875		Am.pedi
AMP9999A	*Amphora* species		Am.sp
SWA0002A	**Aulacoseira ambigua* (Grun. in Van Heurck) Simonsen, 1979		Au.ambi
SWA0005A	**Aulacoseira distans var. distans* (Ehrenb.) Simonsen, 1979		Au.dist
SWA0005E	**Aulacoseira distans var. nivalis* W. Smith) E.Y. Haworth,, 1988		Au.nivalis
SWA0005B	**Aulacoseira distans var. nivaloides* Camburn, 1987		Au.nivaloi
SWA0004A	**Aulacoseira lirata var. lirata* (Ehrenb.) R. Ross in Hartley, 1986		Au.lirata
BRA0006A	**Brachysira brebissonii* R. Ross in Hartley, 1986		B.brebi
BRA00XY1	*Brachysira intermedia* (Østrup) Lange-Bertalot,		B.inter
BRA0010A	*Brachysira neoexilis* Lange-Bertalot, 1994		B.neoex
BRA9999A	*Brachysira* species		B.sp
BRA0005A	*Brachysira zellensis* (Grun.) Round & Mann, 1981		B.zellen
CAL9999A	*Caloneis* species		Cal.sp
CAL0018A	**Caloneis tenuis* Gregory (Krammer), 1985		Cal.ten
CAV00XY2	*Cavinula intractata* (Hust.) Lange-Bertalot,		C.intra
CAV0003A	*Cavinula lacustris* (Greg.) Mann & Stickle, 1990	*Navicula lacustris*	Cav.lacu
CAV00XY1	*Cavinula lapidosa* (Krasske) Lange-Bertalot, 1989		C.lapis
CAV0004A	*Cavinula pseudoscutiformis* (Hust.) Mann & Stickle, 1990	*Navicula pseudoscutiformis*	Cav.pseud
CAV9999A	*Cavinula* species		C.sp
CHM9999A	*Chamaepinnularia* species		Chamae.sp
COC0001C	*Cocconeis placentula var. lineata* (Ehrenb.) Van Heurck, 1885		Co.linea
COC0001A	*Cocconeis placentula var. placentula* Ehrenb., 1838		Co.plance
COC0001B	*Cocconeis placentula var.euglypta* (Ehrenb.) Grun., 1884		Co.eugly
CRA0005A	*Craticula halophila* (Grun. ex Heurck) Mann, 1990	*Navicula halophila*	Cra.halo
CYT0022A	*Cyclotella bodanica* Grunow, in Schneider, 1878		Cy.bodan
CYT0054A	*Cyclotella krammeri* Hakansson, 1990		Cy.kramm
CYT0009A	**Cyclotella ocellata* Pant., 1902		Cy.ocell
CYT0055A	*Cyclotella schumannii* (Grunow) Hakansson, 1990		Cy.schum
CYM0016A	*Cymbella amphicephala* Naegeli ex Kutz., 1849		Cym.amph
CYM0015A	**Cymbella cesatii* (Rabenh.) Grun. in A. Schmidt, 1881		Cym.cesa
CYM0006A	*Cymbella cistula* (Ehrenb. in Hempr. & Ehrenb.) Kirchner, 1878		Cym.cist

Code	Species and Authority	Synonym	Abbreviaton in PCA
CYM0038A	*Cymbella delicatula* Kutz., 1849		Cym.deli
CYM0018A	*Cymbella gracilis* (Rabenh.) Cleve, 1894		Cym.graci
CYM0085A	*Cymbella lapponica* Grun. ex Cleve, 1894		Cym.lappo
CYM0009A	*Cymbella naviculiformis* Auersw. ex Heib., 1863		Cym.navic
CYM9999A	*Cymbella* species		Cym.sp
DID0007A	*Diadesmis perpusilla* (Grun.) Mann, 1990	*Navicula gallica*	Diades.per
DID9999A	*Diadesmis* species		Diades.sp
DIA0002A	**Diatoma hyemale* (Roth) Heib., 1863		D.hyema
DIA0002B	**Diatoma hyemale var. mesodo* (Ehrenb.) Kirchner, 1878	*Diatoma mesodon*	D.mesod
DIP0065A	*Diploneis parma* Cleve, 1891		Dip.parm
ENY0011A	**Encyonema minutum* (Hilse in Rabenhorst) Mann, 1990	*Cymbella minuta*	En.min
ENY0014A	*Encyonema perpusillum*(Cleve) Mann, 1990	*Cymbella perpusilla*	En.perpu
ENY0016A	**Encyonema silesiacum* (Bleisch in Rabenhorst) Mann, 1990	*Cymbella silesiaca*	Cym.silesia
EPI0001A	*Epithemia sorex* Kutz., 1844		Ep. Sor
EUN0013A	**Eunotia arcus* Ehrenb., 1837		E.arc
EUN0070A	*Eunotia bilunaris* (Ehrenb.) F.W. Mills, 1934		E.bilun
EUN0070B	*Eunotia binularis var.mucophila* LB & Norpel, 1991		E.mucoph
EUN00XY1	*Eunotia botuliformis* Wild, Nörpel-Sch. & Lange-Bertalot, 1993		E.botul
EUN0015A	*Eunotia denticulata* (Breb. ex Kutz.) Rabenh., 1864		E.denti
EUN0009A	**Eunotia exigua* (Breb. ex Kutz.) Rabenh., 1864		E.exigu
EUN0108A	*Eunotia intermedia* (Hust) Norpel, Lange-Bertalot & Alles, 1991		E.inter
EUN0114A	*Eunotia muscicola* Krasske, 1939		E.musci
EUN0003A	**Eunotia praerupta* Ehrenb., 1843		E.praer
EUN9999A	*Eunotia* species		E.sp
EUN0105A	*Eunotia subarcuatoides* Alles, Norpel, Lange-Bertalot, 1991		E.subarc
EUN0021A	*Eunotia sudetica* O. Mull., 1898		E.sudet
EUN0045A	*Euntotia nymanniana* Grun. in Van Heurck, 1881		E.nyma
FRA00XY1	*Fragilaria arcus var. recta* Cleve, 1898		F.arcus
FRA0009A	**Fragilaria capucina* Desm., 1825		F.capuc
FRA00XY3	**Fragilaria capucina var. vaucheriae* (Kützing) Lange-Bertalot, 1980		F.vauch
FRA0009M	*Fragilaria capucina var.distans* (Grunow) Lange-Bertalot,		F.distan
FRA0009H	*Fragilaria capucina var.gracilis* (Østrup) Hustedt, 1950		F.gracilis
FRA0002E	*Fragilaria construens var.subsalina* Hust., 1925		F.subsal
FRA0014B	*Fragilaria leptostauron var.dubia* (Grun.) Hust., 1931		F.lepto
FRA0013A	*Fragilaria oldenburgiana* Hust., 1959		Frag.olden
FRA9999A	**Fragilaria* species		F.sp
FRA0070A	**Fragilaria spinarum* L-B & Metzeltin, 1996		F.spina
FRA0060A	**Fragilaria tenera* (W. Smith) Lange-Bertalot, 1980		F.tener
FRA0061A	*Fragilaria zeilleri var.elliptica* Heribaud, 1902		F.zeill
FRF0002A	*Fragilariforma bicapitata* (A. Mayer) Williams & Round, 1988	*Fragilaria bicapita*	F.bicap
FRF0003A	*Fragilariforma constricta* (Ehrenb.) Williams & Round, 1988	*Fragilaria contricta*	F.constric
FRF0001A	*Fragilariforma virescens* (Ralfs) Williams & Round, 1988	*Fragilaria virescens*	F.vires
FRU00XY1	*Frustulia quadrisinuta* Lange-Bertalot, 1996		Fr.quadr
FRU0002A	*Frustulia rhomboides* (Ehrenb.) De Toni, 1891		Fr.rhom
FRU0002K	**Frustulia rhomboides var.crassinervia* (Breb. ex W. Sm.) R. Ross, 1947		Fr.crass
FRU9999A	*Frustulia* species		Fr.sp
GOP0001A	**Gomphoneis olivaceum* (Hornemann) P. Dawson ex R. Ross & Sims, 1978	*Gomphonema olivaceum*	G.oliva
GOP0003A	**Gomphoneis quadripunctatum* (Ostr.) P. Dawson ex R. Ross & Sims, 1978	*Gomphonema olivaceum var.quadripunctatum*	G.quadri
GOM0006A	*Gomphonema acuminatum* Ehrenb., 1832		G.acumin
GOM0020A	*Gomphonema affine* Kutz., 1844		G.affin
GOM0003A	*Gomphonema angustatum* (Kutz.) Rabenh., 1864		G.angusta
GOM0073A	**Gomphonema angustum* Agardh, 1831		G.angust
GOM0030A	*Gomphonema auritum* A. Braun ex Kutz., 1849		G.aurit
GOM0029A	*Gomphonema clavatum* Ehr., 1832		G.clavat
GOM0024A	**Gomphonema clevei* Fricke in A. Schmidt, 1902		G.clevei
GOM0004A	*Gomphonema gracile* Ehrenb., 1838		G.gracil
GOM00XY1	**Gomphonema minutiforme* Lange-Bertalot & Reinchardt,		G.minuti
GOM0015A	*Gomphonema montanum* Schum., 1867		G.montan
GOM0001F	**Gomphonema olivaceum var.olivaceoides* (Hust.) L-B, 1989		G.olivaceoid
GOM0013A	**Gomphonema parvulum* (Kutz.) Kutz., 1849		G.parvu
GOM9999A	**Gomphonema* species		G.sp
GOM0011A	*Gomphonema subclavatum* (Grun. in Schneider) Grun. in Van Heurck, 1880		G.subcla
GOM0025H	*Gomphonema vibrio* Ehrenb., 1843		G.vibri
HAT9999A	*Hantzschia* species		Han.sp

Code	Species and Authority	Synonym	Abbreviaton in PCA
NAV0037A	*Navicula angusta* Grun., 1860		N.angusta
NAV0007A	*Navicula cryptocephala* Kutz., 1844		N.crypt
NAV00XY1	*Navicula lesmonensis* Hust., 1957		N.lesmo
NAV0537A	*Navicula notha* Wallace, 1960		N.notha
NAV0003A	*Navicula radiosa* Kutz., 1844		N.radio
NAV0008A	**Navicula rhyncocephala* Kutz., 1844		N.rhyn
NAV0090A	*Navicula rotunda* Hust., 1945		N.rotun
NAV0133A	*Navicula schassmannii* Hust., 1937		N.schass
NAV9999A	*Navicula* species		N.sp
NAV0114A	*Navicula subrotundata* Hust., 1945		N.subrot
NAD00XY1	*Naviculadicta pseudostauron* Lange-Bertalot, 1996		Nav.pseudo
NAD9999A	*Naviculadicta* species		Nav.spp
NEI9999A	*Neidium* species		Neid.sp
NIT0202A	*Nitzschia alpina* Hustedt, 1943		Ni.alpi
NIT0002A	*Nitzschia fonticola* Grun. in Van Heurck, 1881		Ni.fonti
NIT0009A	*Nitzschia palea* (Kutz.) W. Sm., 1856		Ni.palea
NIT0005A	*Nitzschia perminuta* (Grun. in Van Heurck) M. Perag., 1903		Ni.permi
NIT9999A	*Nitzschia* species		Ni.sp
PIN0008A	*Pinnularia divergens* W. Sm., 1853		P.divergens
PIN0016A	**Pinnularia divergentissima* (Grun.in Van Heurck) Cleve, 1896		P.diverg
PIN0006A	*Pinnularia mesolepta* (Ehrenb.) W. Sm., 1853		P.meso
PIN0011A	*Pinnularia microstauron* (Ehrenb.) Cleve, 1891		P.micro
PIN0180A	*Pinnularia neomajor* Krammer, 1992		P.neom
PIN9999A	*Pinnularia* species		P.sp
PIN0161A	*Pinnularia subrostrata* (A. Cleve) A. Cleve-Euler, 1955		P.subrost
PIN0056A	*Pinularia rupestris* Hantzsch in Rabenh., 1861		P.rupes
PTH0003A	*Planothidium lanceolata* (Breb.) Round & Bukhtiyarova	*Achnanthes lanceolata*	P.lance
PST0012A	**Psammothidium marginulata*(Grun.) Round & Buktiyarova	*Achnanthes marginulata*	Ps.margin
PST00XY1	**Psammothidium scoticum* (Flower & Jones, 1989) L. Bukhtiyarova & F.E. Round, 1996	*Achnanthes scotica*	Ps.scoti
PST0005A	**Psammothidium subatomoides* (Hustedt) L. Bukhtiyarova & F.E. Round, 1996	*Achnanthes subatomoides*	Ps.subat
PSE0002A	**Pseudostaurosira pseudoconstruens* (Marciniak) Williams & Round, 1987	*Fragilaria pseudoconstruens*	Pse.speudo
PSE00XY1	*Pseudostaurosira robusta* (Fusey) D.M. Williams & Round, 1987	*Fragilaria robusta*	Pse.robus
REI0001A	**Reimeria sinuata* (Greg.) Kociolek & Stoermer, 1987	*Cymbella sinuata*	Rei.sinu
ROS0001A	*Rossithidium linearis* (W.Sm.) Round & Bukhtiyarova	*Achnanthes linearis*	R.linear
SEL0001A	*Sellaphora pupula* (Kutz.) Mereschkowsky, 1902		Sella.pup
SEL0007A	*Sellaphora rectangularis* (Greg.) L-Bertalot,		Sell.rec
SEL0002A	*Sellaphora seminulum* (Grun.) Mann, 1990	*Navicula seminulum*	Sel.seminu
SEL9999A	*Sellaphora* species		Sella.sp
STA0001A	**Stauroforma exiguiformis* (Lange-Bertalot) Flower, Jones & Round, 1996	*Fragilaria exigua*	F.exig
STR9999A	*Stauroneis* species		Stauro.sp
STS0001B	**Staurosira construens var. venter* (Grun.) Williams & Round	*Fragilaria construens var.venter*	Stau.venter
STS0001C	*Staurosira contruens var. binodis* (Ehrenb.) Hamilton	*Fragilaria construens var.binodis*	Stau.binod
STS0002A	**Staurosira elliptica* (Schumann) Williams & Round, 1987	*Fragilaria elliptica*	St.ellip
STL0002A	*Staurosirella pinnata* (Ehrenb.) Williams & Round, 1987	*Fragilaria pinnata*	Sta.pinna
STP0005A	*Stenopterobia delicatissima* (Lewis) M. Perag., 1897		Steno.deli
SUR0010A	*Surirella robusta* Ehrenb., 1840		Suri.robu
SUR9999A	*Surirella* species		Suri.sp
SUR0007A	*Surirella tenera* Greg., 1856		Suri.tene
SYN0007B	*Synedra amphicephala var. austriaca* (Grun. in Van Heurck) Hust., 1932	*Fragilaria gracillicima*	Sy.amphi
SYN0004A	**Synedra parasitica var. parasitica* (W. Sm.) Hust., 1930	*Fragilaria parasitica*	Sy.paras
TAL0001A	**Tabellaria flocculosa* (Roth) Kutz., 1844		Tab.flocc
TET00XY1	*Tetracyclus glans* (Ehrenb.) F.W. Mills, 1935		Tetra.glan